Electrochimica Acta 56 (2011) 6932–6939

Contents lists available at ScienceDirect

Electrochimica Acta

journal homepage: www.elsevier.com/locate/electacta

# Hydrothermal growth of $Sn^{4+}$-doped $FeS_2$ cubes on FTO substrates and its photoelectrochemical properties

Jian Xia, Xihong Lu, Wei Gao, Jiqing Jiao, Huajie Feng, Liuping Chen*

*School of Chemistry and Chemical Engineering, Sun Yat-sen University, Guangzhou, Guangdong 510275, People's Republic of China*

ARTICLE INFO

*Article history:*
Received 10 February 2011
Received in revised form 4 June 2011
Accepted 4 June 2011
Available online 14 June 2011

*Keywords:*
$Sn^{4+}$-doped $FeS_2$ cubes
Thin films
Hydrothermal process
Formation process
Photoelectrochemical properties

ABSTRACT

$Sn^{4+}$-doped $FeS_2$ cubes with high yield thin films have been successfully synthesized on FTO glass through a simple hydrothermal process. The $Sn^{4+}$-doped $FeS_2$ cubes are single crystalline in cubic structure with (2 0 0) facet as the main exposed surface. The formation process was investigated. $Sn^{2+}$ was found to play an important role during the formation process of $FeS_2$ growing on FTO glass. The direct optical band gap value can be estimated to be 1.71 eV which is much larger than that of bulk $FeS_2$ due to the $Sn^{4+}$ doping. The photoelectrochemical properties of the $Sn^{4+}$-doped $FeS_2$ films were studied as well. There is a significant increase in photocurrent of $Sn^{4+}$-doped $FeS_2$ electrode compared to that of undoped sample.



## 1. Introduction

Pyrite ($FeS_2$) with an optical energy band gap of 0.95 eV has attracted much interest in both fundamental research and practical applications due to its inherent advantages such as environmental compatibility, excellent electron mobility, large optical absorption coefficient ($\lambda \leq 700$ nm, $\alpha \geq 5 \times 10^5$ $cm^{-1}$), non-toxic and high quantum efficiency (>80%) [1,2]. During the past few years, much effort has been made to synthesize $FeS_2$ nanostructures and great advances have been achieved. Various $FeS_2$ nanostructures such as nanorods [3], nanowebs [4], nanowires [5] and nanosheets [6] have been synthesized and found to have charming performances in lithium ion batteries [7,8], high-energy-density batteries [9], photocatalysis [2], and solar energy conversion [10]. Until now, many methods have been put forward to fabricate $FeS_2$ thin films including metal organic chemical vapor deposition (MOCVD) [11,12], microwave irradiation [13], electrodeposition [14], sulfurization of iron films [15], and reactive magnetron sputtering [16], etc. However, these synthesized approaches often not only require relatively large energy consumption, special equipment, complicated subsequent processes, but also exhibit poor control and reproducibility. In addition, these prepared films often have been found to be sulfur deficient, with a $FeS_{2-x}$ or orthorhombic marcasite $FeS_2$ phase which may greatly restrict their application performance even with trace amounts [17].

Hydrothermal synthesis has been a well-established and promising approach for preparing controlled inorganic materials. Fundamentally, it provides a clean, high-yield, high-crystalline, and always low temperature, low-cost and environmental friendly method compared with conventional solid state or vapor reactions [18,19]. During the past decade, several groups have focused on hydrothermal synthesis of $FeS_2$ and remarkable progress has been made [17,20–22]. Chen's group synthesized cubic $FeS_2$ crystallites via a single-source hydrothermal approach using iron diethyldithiocarbamate as precursor and found it delivered a large discharge capacity which might find possible application in lithium cells [21]. Wadia et al. used a single-source molecular precursors and surfactant-assisted hydrothermal method and successfully synthesized single phase pyrite $FeS_2$ nanocrystals which represented a good candidate material for studies of nanoscale photovoltaic solar cells [17]. More recently, Wang and his co-workers [22] developed a facile surfactant-assisted ethylene glycol-mediated solvothermal approach which allowed to select synthesis of uniform $FeS_2$ octahedral and cubic crystallites by simply changing reaction parameters such as NaOH concentration, surfactants, etc. However, these synthesized routes are not only dependent upon particular molecular precursors or reagents, but also provide powder products which are difficult to use as thin film-based materials for photoelectric devices.

In this paper, uniform $Sn^{4+}$-doped $FeS_2$ films with single crystallinity have been synthesized via a hydrothermal approach. Particularly, to the best of our knowledge, hydrothermal growth of $FeS_2$ or its compounds on FTO substrates have not been reported yet. Compared with $FeS_2$ powder, a small shift could be observed in

* Corresponding author. Tel.: +86 20 8411 5559; fax: +86 2084112245.
*E-mail address:* cesclp@mail.sysu.edu.cn (L. Chen).

0013-4686/$ – see front matter © 2011 Elsevier Ltd. All rights reserved.
doi:10.1016/j.electacta.2011.06.021

both XRD and Raman spectrum due to the reduction of the lattice spacing. The optical properties were investigated by UV–vis–NIR spectroscopy and an obvious blue-shift was observed. Moreover, compared with pure $FeS_2$ electrodes, the $Sn^{4+}$-doped $FeS_2$ thin film electrode had a better photoelectric performance which might lead them more suitable for photoelectrical materials.

## 2. Experimental

### 2.1. Materials

All reagents including $FeCl_2{\cdot}7H_2O$, $SnCl_2{\cdot}2H_2O$, $Na_2S_2O_3{\cdot}5H_2O$, sulfur powders, polyethylene glycol (PEG), sodium dodecyl sulfate (SDS), polyvinyl pyrrolidone (PVP), tartaric acid, sodium hydroxide and ethanol were analytical grade and used without any further purification. The fluorine-doped tin oxide (FTO) conductive glasses were cleaned ultrasonically with diluted hydrochloric acid, ethanol, acetone, and deionized water, respectively, and then dried with an electric hair dryer.

### 2.2. Synthesis

In a typical procedure, 0.278 g $FeCl_2{\cdot}7H_2O$, 0.248 g $Na_2S_2O_3{\cdot}5H_2O$, 0.112 g $SnCl_2{\cdot}2H_2O$, 0.032 g sulfur powders and 0.1 g PEG were dissolved in a mixture composed of 19 mL 0.1 mol/L sodium tartrate – tartaric acid buffer solution (pH 3) and 5 mL ethanol at room temperature with a 30 mL Teflon-lined autoclave. Afterward, a piece of FTO glass (2.5 cm × 1 cm) was placed with an angle against the wall of the Teflon-liner with the conducting side facing down. The hydrothermal synthesis was conducted at 220 °C for 24 h in an electric oven. When the reaction was finished, the autoclave was cooled down to room temperature naturally. Finally, the FTO glass was taken out, washed thoroughly with distilled water, carbon disulfide and ethanol for several times and dried in vacuum oven at 60 °C for 6 h for further characterization. $FeS_2$ powder was synthesized in a similar way with the absence of $SnCl_2{\cdot}2H_2O$.

### 2.3. Preparation of the electrodes

$Sn^{4+}$-doped $FeS_2$ electrodes were prepared directly from $Sn^{4+}$-doped $FeS_2$ films with the active area of 0.4 cm × 0.4 cm and weight of 0.6 mg. $FeS_2$ electrode was prepared from $FeS_2$ powder. For comparison, we also scraped $Sn^{4+}$-doped $FeS_2$ off the FTO glass and made $Sn^{4+}$-doped $FeS_2$ powder electrode. The fabricated process of the electrodes was similar to what was described by Shi et al. [23] and expatiated as follows. First, the powder and a few drops of ethanol were added in a 5 mL beaker and ultrasonically dispersed until a homogeneous milk-like suspension was obtained. Then, the suspension was daubed on FTO glass surface with an active area of 0.4 cm × 0.4 cm. The resulting films were dried in vacuum at 60 °C for 3 h for further use.

### 2.4. Characterization

The prepared films were characterized by X-ray diffractometer (XRD, D8 ADVANCE), field emission scanning electron microscopy (FE-SEM, JSM-6330F), energy dispersive spectroscopy (EDS, FEI/Quanta 400), transmission electron-microscopy (TEM, JEM2010-HR), the X-ray photoelectron spectroscopy (XPS, ESCALAB 250), laser micro-raman spectrometer (Renishaw inVia), respectively. The optical properties of the films were measured with a UV–vis–NIR Spectrophotometer (UV, Shimadzu UV-3150). The photoelectrochemical properties were carried out in a standard three-electrode configuration using CHI 750a electrochemical workstation (Chenhua, Shanghai) with a photoanode ($FeS_2$ or $Sn^{4+}$-doped $FeS_2$ film), a cathode (graphite rod) and a saturated calomel electrode (SCE) as the reference electrode which was connected to the cell with a double salt bridge system. An aqueous solution of 0.1 mol/L $Na_2SO_3$ was utilized as the supporting electrolyte. The working electrode was illuminated with a xenon lamp (PLS-LAX500, Beijing Changtuo) with illumination intensity of 50 mW $cm^{-2}$.

## 3. Results and discussion

The phase of the as-prepared $Sn^{4+}$-doped $FeS_2$ films were determined by XRD shown in Fig. 1b. All the peaks can be well indexed as cubic pyrite $FeS_2$ (JCPDS Card No. 42-1340) with the lattice parameter $a$ = 5.418 Å. The (2 0 0) diffraction peak is much stronger than that of $FeS_2$ powder (XRD pattern in Fig. 1a), indicating the (2 0 0) planes may be the main exposed surface. Moreover, compared with $FeS_2$ powder in Fig. 1a, a slight shift (about 0.1°) to higher degree can be observed. This may be due to the lattice constriction effect resulting from $Sn^{4+}$ doping. As we know, the ionic radius of $Sn^{4+}$ (71 pm) is a little smaller than that of $Fe^{2+}$ (76 pm). It is expected that $Sn^{4+}$ ions can replace lattice $Fe^{2+}$ in $FeS_2$ and, accordingly, occupy the lattice $Fe^{2+}$ positions [24,25]. Therefore, the lattice constriction upon $Sn^{4+}$ doping will happen spontaneously and lead to the shift of the diffraction peaks.

X-ray photoelectron spectra (XPS) analyses were carried out to investigate the surface electronic states of the $Sn^{4+}$-doped $FeS_2$ films. The broad scan of the particle surface in Fig. 2a shows that the sample consists of iron, tin, sulfur, oxygen, and carbon. The weak C1s and O1s peaks come from the adsorbed reactants and gaseous molecules in the atmosphere. Two strong peaks at 487.1 and 495.5 eV in Fig. 2b can be indexed to $Sn3d_{3/2}$ and $Sn3d_{5/2}$, respectively. These values agree with the reported data of $Sn^{4+}$ [26]. Fig. 2c presents the Fe2p spectra. The peaks located at 707.4 eV and 720 eV correspond to $Fe2p_{3/2}$ and $Fe2p_{1/2}$ which are in agreement with the literature values of bulk $FeS_2$ [13,17,27]. The middle peak at 717 eV in Fig. 2c attributes to electronic states of Sn3p. The S2p

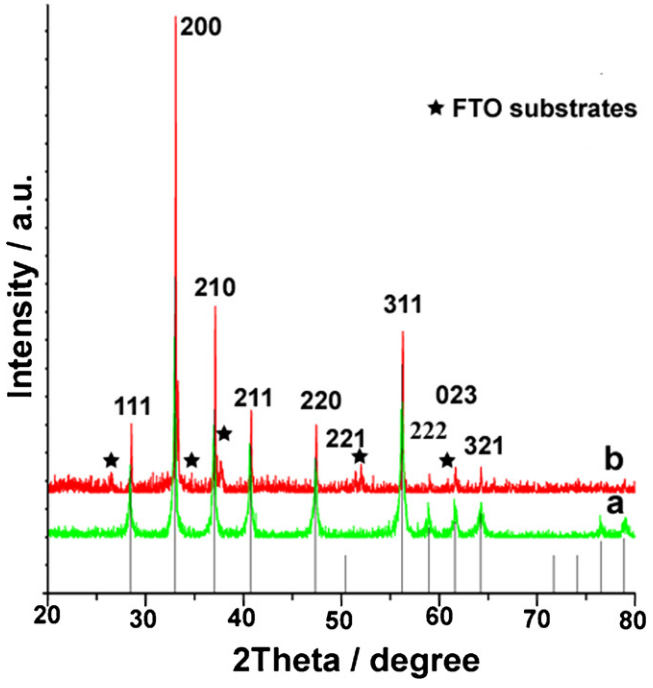


**Fig. 1.** XRD patterns of the as-prepared products: (a) $FeS_2$ powder, and (b) $Sn^{4+}$-doped $FeS_2$ film.